Influence of Nano-structured Alumina Coating on Composite-Zirconia Bonding and its Characterization

Putsadeeporn Thammajaruk[a] / Supanee Buranadham[b] / Ornnicha Thanatvarakorn[c] / Massimiliano Guazzato[d]

Purpose: To compare microtensile bond strength and characterize the bond of nano-structured alumina-coated vs tribochemically silica-treated zirconia specimens.

Materials and Methods: Eight zirconia blocks were assigned to two groups: nano-structured alumina coating (AIN) and tribochemical silica treatment (CoJet) followed by RelyX Ceramic Primer (COJ). For each group, two identically pre-treated zirconia blocks were bonded with RelyX Unicem 2 Cement and cut into 30 stick-shaped specimens (1 x 1 x 9 mm^3). A total of 120 specimens were stored in distilled water at 37°C for 24 h and then assigned to three groups (n = 20/test group): short-term test, thermocycling 5000 cycles, and thermocycling 10,000 cycles. The specimens were tested in tensile mode. The bond strength results were analyzed using two-way ANOVA, followed by one-way ANOVA and Tukey's HSD ($\alpha = 0.05$). Failure mode and surfaces were analyzed with optical microscopy and SEM. FTIR and EDS were used for chemical analyses on primer-, mechanically and/or chemically pre-treated surfaces.

Results: The mean bond strengths of AIN and COJ groups were not statistically significantly different in all aging conditions ($p > 0.05$). Thermocycling significantly decreased the bond strength of both groups ($p < 0.01$). The AIN groups exhibited predominantly either adhesive or mixed failure, whereas the specimens in the COJ groups mainly presented either mixed or cohesive failure in composite cement. Silane chemically reacted with mechanically pre-treated COJ surface via the absorption of Si-O group.

Conclusion: The composite-zirconia bond strength after application of a nano-structured alumina coating was comparable to that after tribochemical silica treatment.

Keywords: zirconia, tribochemical silica coating, nano-structured alumina coating, surface treatment, composite cement, microtensile bond strength, surface characterization.

J Adhes Dent 2018; 20: 233–242.
doi: 10.3290/j.jad.a40512

Submitted for publication: 14.12.17; accepted for publication: 09.04.18

The use of indirect zirconia restorations has increased significantly over the last few years due to their superior mechanical and optical properties when compared to glass ceramics and metal alloys, respectively.[7,8] However, the clinical success rate of zirconia restorations is compromised in those situations where bonding to tooth structure does not rely on the resistance and retention form of the preparation and mechanical retention is minimal, for example, in occlusal veneers, partial coverage restorations, or resin-bonded fixed dental prostheses.[19]

Zirconia conditioning techniques have been developed with the purpose of achieving long-term durable bond strength via a mechanical interlocking of composite cement and chemical interaction between pre-treated surfaces and functional monomers such as 10-methacryloyloxydecyl dihydrogenphosphate (10-MDP), or a methacrylate phosphoric-ester group in the primer or composite cement.[13] One of the most effective surface pre-treatment techniques for zirconia bonding is based on the use of tribochemical silica treatment followed by application of a silane coupling agent.[13] The use of air abrasion favors bonding by increasing the surface area and roughness, while the use of silane increases bonding efficacy to silica-treated zirconia via the formation of siloxane bonds.[23,29] However, previous studies have reported contradictory results regarding the short- and long-term bond strength. According to these studies, the

[a] *PhD Student, Department of Bioengineering, The University of Sydney, New South Wales, Australia. Conception, design, data acquisition, analysis and interpretation, drafted and critically revised the manuscript in partial fulfillment of requirements for a PhD.*

[b] *Clinical Lecturer, Department of Prosthetic Dentistry, Prince of Songkla University, Songkhla, Thailand. Conception, design, data analysis, critically revised the manuscript.*

[c] *Clinical Lecturer, Department of Operative Dentistry, Bangkokthonburi University, Bangkok, Thailand. Data analysis, interpretation, critically revised the manuscript.*

[d] *Associate Professor, Discipline of Prosthodontics, The University of Sydney, New South Wales, Australia. Conception, design, data analysis, interpretation, critically revised the manuscript.*

Correspondence: *Putsadeeporn Thammajaruk, The University of Sydney, Faculty of Dentistry, Department of Bioengineering, Level 2, Westmead Center of Oral Health, Darcy Road, Westmead, NSW, 2145, Australia. Tel: +61-451-988-707; e-mail: ptha8204@uni.sydney.edu.au*

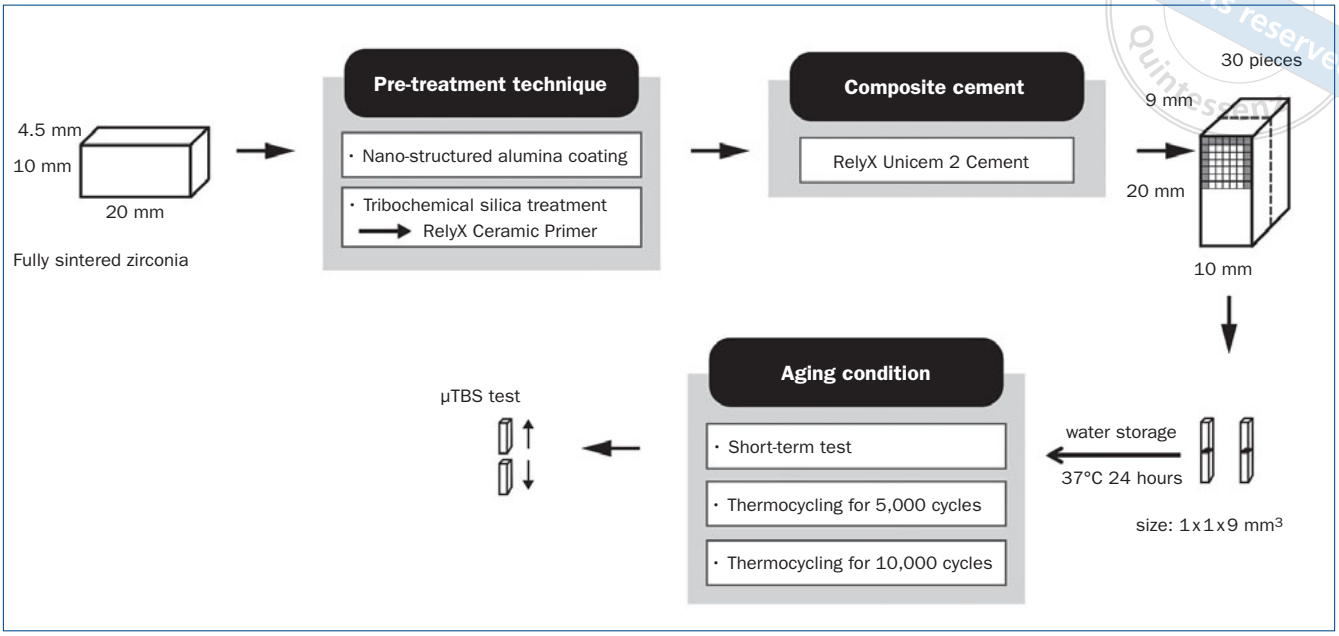

Fig 1 Schematic figure of the study design.

short-term bond strength of tribochemical silica-treated zirconia and composite cement was improved, while the long-term bond strength was stable or significantly decreased following thermocycling or long-term water storage.[34,35]

More recently, a technique based on nano-structured alumina coating of zirconia has been proposed with the objective of improving bond strength and durability.[17] This technique is based on the hydrolysis of aluminum nitride powder on the zirconia surface and the formation of a thin alumina coating approximately 240 nm thick on the fitting surface.[17] It has been speculated that this alumina coating forms a strong bond to zirconia and its surface topography facilitates micromechanical retention to composite cement, providing higher bond strength and durability.[17] However, there is little information on the bond characterization and the short- and long-term bond strength of this technique when compared with a conventional protocol where chemical and mechanical treatments are used.[17,21]

Hence, the aims of this study were to compare the microtensile bond strength and characterize the nature of the bond of alumina-coated vs tribochemically silica-treated zirconia specimens. The hypotheses tested were: (1) nano-structured alumina coating would result in significantly higher bond strength and (2) thermocycling would decrease the bond strength in both tested groups.

MATERIALS AND METHODS

Specimen Preparation and Mechanical Surface Pre-treatment

The study design is schematically shown in Fig 1. Eight zirconia blocks (13 x 26 x 5.9 mm^3) were fabricated from pre-sintered zirconia disks (GC Initial Zirconia HT Disk, GC Europe; Leuven, Belgium) by CAD/CAM process using a milling machine (Roland DWX-50, Roland DG; Shizuoka-ken, Japan). Following milling, the zirconia blocks were sintered in a furnace (Vita Zyrcomat 6000MS, Vita Zahnfabrik; Bad Säckingen, Germany) for 2 h at 1450°C as recommended by the manufacturer. After sintering, the zirconia blocks (10 x 20 x 4.5 mm^3) were ultrasonically cleaned for 10 min each in acetone and distilled water. The blocks were then randomly and equally assigned to two groups, AlN and COJ. The blocks of group AlN were immersed in the diluted aqueous suspension of aluminum nitride powder at 75°C for 15 min. Then the coated surfaces were air dried in an oven for 2 h at 110°C and thermally treated by heating in an electric resistance furnace at 900°C for 1 h.[17]

One of the largest surfaces of each block of COJ group was air abraded with 30-μm silica-coated aluminum oxide particles (CoJet, 3M Oral Care; St Paul, MN, USA) at 0.25 MPa for 40 s. Residual abrasive materials were removed with an oil-free air syringe. Silane (RelyX Ceramic Primer, 3M Oral Care) was then applied on the mechanically pre-treated surface.

Microtensile Bond strength (μTBS) Testing

Two identically pre-treated zirconia blocks were bonded together using composite cement (RelyX Unicem 2 Automix, 3M Oral Care) under a constant load of 750 g. Excess cement was removed with cotton pellets. Light polymerization was initiated with a halogen light-curing unit (output of 850 mW/cm^2) (Optilux 501, Kerr; Orange, CA, USA) for 20 s on each of the 6 sides of the bi-layered zirconia blocks, followed by self-polymerization for 10 min. Each bi-layered zirconia block was sectioned using a water-cooled diamond saw (Isomet 4000,

Table 1 Results of two-way ANOVA with the independent variables surface pre-treatment and aging, and dependent variable microtensile bond strength

Source	Sum of Squares	df	Mean Square	F	Sig.
Corrected model	4576.099[a]	5	915.220	3.625	0.004
Intercept	751180.629	1	751180.629	2975.058	0.000
Surface pre-treatment	20.891	1	20.891	0.083	0.774
Aging	4496.182	2	2248.091	8.904	0.000
Surface pre-treatment x aging	59.027	2	29.513	0.117	0.890
Error	28784.173	114	252.493		
Total	784540.902	120			
Corrected total	33360.273	119			

[a] $R^2 = 0.137$ (adjusted $R^2 = 0.099$).

Buehler; Lake Bluff, IL, USA) at low speed (600 rpm, feed rate 4 mm/min) into stick-shaped specimens with a cross section at the bonding interface of ca 1.0 x 1.0 mm^2. Thirty sticks were obtained from each zirconia block (n = 60/group).

All specimens were stored in distilled water at 37°C for 24 h, then the specimens were equally assigned to 3 aging conditions (n = 20/test group): short-term[14] (no additional treatment following water storage), thermocycling 5000 cycles, and thermocycling 10,000 cycles between 5°C (± 2°C) and 55°C (± 2°C) with a 30-s dwell time and a 10-s transfer time.

After the designated aging period, the specimens were subjected to μTBS with a universal testing machine (LRX-Plus, Lloyd Instruments; Hampshire, UK) at a speed of 1 mm/min until failure occurred. The Shapiro-Wilk test indicated that the normality assumption for the bond strength data was satisfied. The bond strength data were statistically analyzed using two-way ANOVA followed by one-way ANOVA and Tukey's HSD as post-hoc comparisons. All statistical analyses were performed at a 5% significance level with SPSS software (IBM v. 24.0, IBM; Armonk, NY, USA).

Failure Mode Analysis

The fractured specimens were observed under a light microscope (Olympus BX 60, Olympus; Tokyo, Japan) at 50X magnification and field-emission scanning electron microscope (FE-SEM, Zeiss Sigma VP FEG SEM, Carl Zeiss; Jena, Germany) to identify the type of failure, as follows:[25]

- Type 1: adhesive failure (80% to 100% of the failure occurred at the interface between composite cement and zirconia).
- Type 2: cohesive failure (80% to 100% of the failure occurred within composite cement or zirconia).
- Type 3: mixed failure (mixed adhesive and cohesive failure patterns in the same specimen).

Weibull Statistics

The μTBS was analyzed by Weibull distribution (Minitab Software V.18; State College, PA, USA). Weibull parameters (Weibull characteristic strength at 63.2% probability of failure and Weibull modulus) were computed by maximum-likelihood estimation, whereas 95% confidence intervals (CIs) were calculated with Parametric Distribution Analysis (Right Censoring). The significant difference in test groups was compared using Weibull parameters and 95% CIs.

Morphology of Pre-treated Surfaces

Additional blocks for each group were observed with an FE-SEM (gold coated, 10^{-5} mbar pressure, 15 kV energy range, 85 μA beam current, at either 1000X or 40,000X, secondary electron image) to assess surface topography following mechanical pre-treatment (n = 3).

The specimens from the outside layer of each group which were not used to measure the bond strength were observed with FE-SEM to measure the thickness of the cement layer.

Chemical Characterization

Elemental composition on the as-sintered zirconia, alumina-coated zirconia surfaces, and tribochemically silica-treatment surfaces (with and without primer conditioning, n = 1) was analyzed using energy dispersive x-ray spectroscopy (EDS) with a 20-kV energy range and 85-μA beam current at 150X (secondary electron image) (EDS Software-AZtecEnergy, Oxford Instruments; High Wycombe, UK).

Infrared spectra were collected using a Fourier-Transform Infrared (FTIR) spectrometer (Bruker ALPHA portable spectrometer, Bruker; Karlsruhe, Germany) equipped with a single-reflection diamond-attenuated total-reflection (ATR) module and deuterated triglycine sulphate (DTGS) detector. Spectra were collected on primer alone (as a reference) and the primed COJ mechanically pre-treated surfaces in ambient conditions from 300 cm^{-1} to 4000 cm^{-1} with a resolution of 4 cm^{-1}, 256 sample scans, and air background (n = 1). Ranges between 780 cm^{-1} and 1280 cm^{-1} in the spectrum of primer and primed COJ specimens were analyzed using pseudo-Voigt function with a constant profile factor of 0.5.

Table 2 The results of bond strength, Weibull analysis, and failure mode (n = 20/test group)

Group	Storage	Bond strength in MPa (SD)*,**	Weibull modulus (95% confidence interval)***	Weibull characteristic strength in MPa (95% confidence interval)***	Failure analysis		
					Ad	Co	Mixed
COJ	24 h	85.10 (15.68) aA	7.16 (5.01–10.23) PQ	91.07 (85.42–97.09) XY	–	65%	35%
	TC 5000	80.56 (17.12) abB	4.90 (3.58–6.69) P	87.40 (79.48–96.10) XY	20%	30%	50%
	TC 10,000	70.45 (19.85) bC	4.30 (3.00–6.17) P	77.61 (69.73–86.37) X	10%	30%	60%
AIN	24 h	87.18 (10.22) xA	10.70 (7.56–15.13) Q	91.44 (87.58–95.47) Y	50%	–	50%
	TC 5000	79.43 (14.60) xyB	6.54 (4.60–9.28) PQ	85.36 (79.53–91.61) XY	50%	–	50%
	TC 10,000	72.00 (16.27) yC	5.17 (3.66–7.29) P	78.34 (71.63–85.68) X	55%	–	45%

*Different lower-case letters in one column indicate significant differences among aging conditions in the same group. **Different upper-case letters in one column indicate significant difference between COJ and AIN in each aging condition. ***Different upper-case letters in one column indicate significant difference among groups and subgroups (no overlapping). Ad: adhesive failure; Co: cohesive failure in composite cement. TC: thermocycling between 5°C (±2°C) and 55°C (±2°C) with 30-s dwell time and 10-s transfer time.

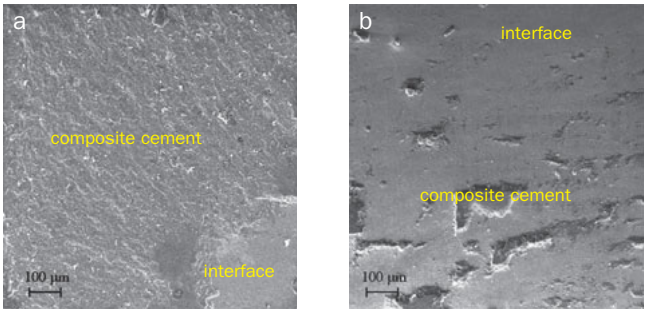

Fig 2 SEM images illustrating the fracture surface of COJ and AIN specimens: a: cohesive failure of COJ specimen; b: adhesive failure of AIN specimen.

Phase Transformation Analysis

Mechanically pre-treated AIN and COJ surfaces and as-sintered zirconia were examined using x-ray diffraction (XRD, Diffractometer D5000, Siemens; Karlsruhe, Germany) to quantify the relative amount of the monoclinic phase. XRD data were collected with Cu Kα radiation from 2θ = 25 to 35 with a step size of 0.02 degrees and with a 1-s step interval (n = 3). The equation suggested by Garvie and Nicholson was used to calculate the relative amount of monoclinic phase.[6]

The depth of the *t-m* transformed layer was determined by focused ion-beam SEM (FIB-SEM) (gold coated, 10^{-5} mbar pressure, 30 kV energy range, 1 nA beam current, at either 10,000X or 11,000X, InLenS image) (Zeiss Auriga FIB-SEM, Carl Zeiss) following mechanical pre-treatment (n = 3).

RESULTS

Microtensile Bond Strength (µTBS) Testing

The two-way ANOVA of microtensile bond strengths is shown in Table 1. Means and standard deviations (SD) of the µTBS of AIN and COJ groups under the three aging conditions are presented in Table 2. The mean µTBS of AIN groups was not statistically significantly different from the COJ groups under any aging conditions ($p > 0.05$). Thermocycling significantly decreased the µTBS in both AIN and COJ groups ($p < 0.05$).

Failure Mode Analysis

AIN groups predominantly exhibited either mixed or adhesive failure, whereas most of the specimens in COJ groups presented either mixed or cohesive failure in composite cement (Table 2 and Fig 2).

Weibull Analysis

The Weibull parameters and Weibull plots are shown in Table 2 and Fig 3, respectively. The Weibull characteristic strength and Weibull modulus of AIN and COJ groups were not significantly different when compared in each aging condition.

Morphology of Pre-treated Surfaces

SEM images of mechanically pre-treated AIN and COJ surfaces are shown in Fig 4. Images of the alumina-coated surface showed the presence of elongated alumina crystals measuring approximately 200 nm x 40 nm. SEM images of tribochemically silica-treated zirconia specimens showed the typical abraded topography with clusters of nano-silica particles.

The cement thickness was approximately 17 µm in AIN group, while it was around 23 µm in the COJ group.

Chemical Characterization (EDS and FTIR)

Zr and O were the major elements found on the as-sintered zirconia, mechanically pre-treated AIN and COJ surfaces, whereas Si was additionally found on COJ surfaces. An even distribution of the elements in both mechanically pre-treated groups was detected. Upon primer application in the latter group, higher percentages of Si, C, and O were detected (Table 3).

The FTIR spectra are shown in Fig 5. Fitting parameters are given in Table 4.

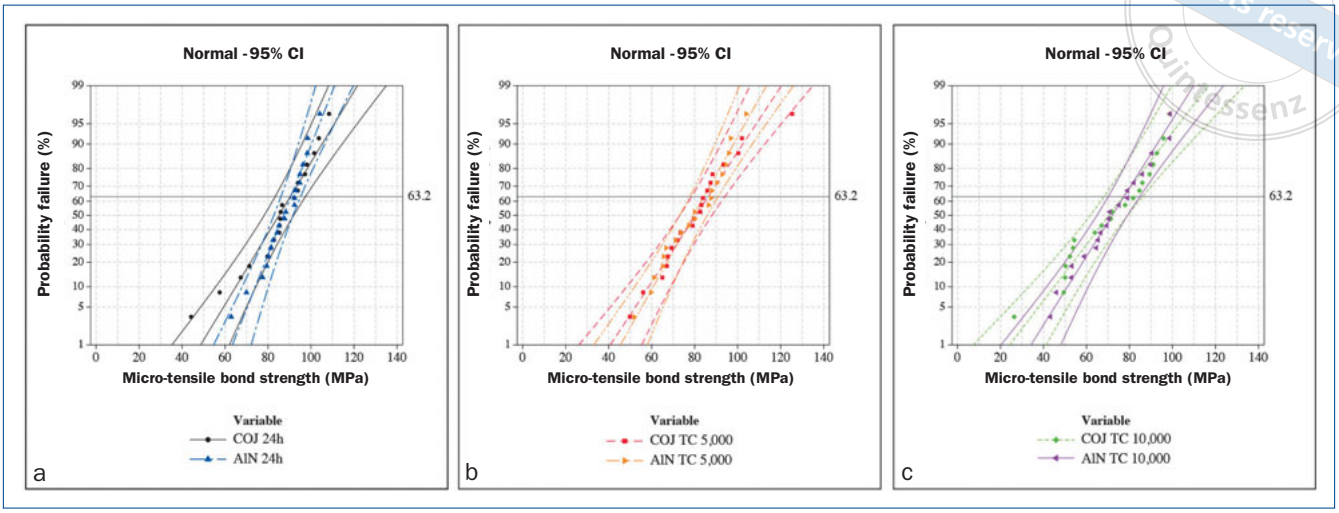

Fig 3 Graph illustrating the Weibull analysis for the different pre-treatment techniques: a: 24-h water storage; b: thermocycling 5000 cycles; c: thermocycling 10,000 cycles.

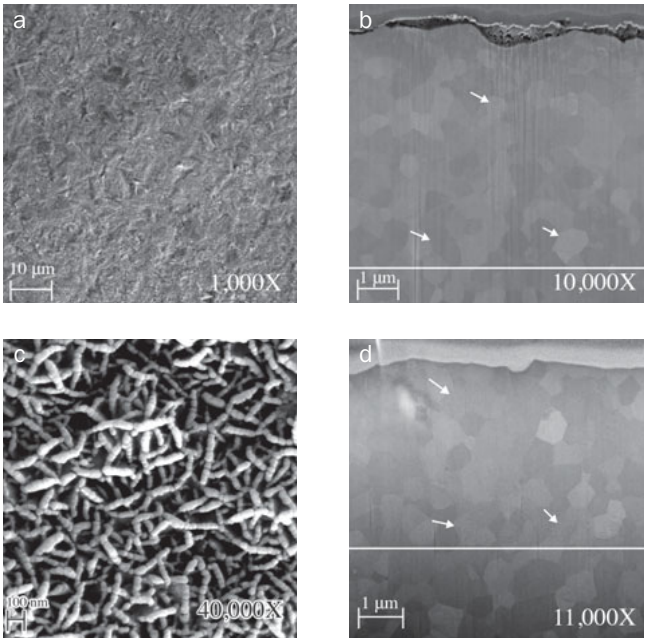

Fig 4 FE-SEM image of surface topography of a mechanically pre-treated zirconia and an FIB-SEM image of cross-sectional surface topography of a mechanically pre-treated zirconia surface. a and b: tribochemical silica treatment; c and d: nano-structured alumina coating. The white line indicates an estimate of the *t-m* transformed layer border. White arrows show facetting of the zirconia grains, indicating *t-m* phase transformation.

Phase Transformation Analysis (XRD and FIB-SEM)

The XRD analyses show the major peaks of the tetragonal and monoclinic phases of zirconia (Fig 6). XRD analysis quantified the percentage of monoclinic phase transformation of as-sintered zirconia as 3.33% and for the mechanically pre-treated AlN surface as 4.21%, whereas it was 6.16% for COJ. Cross-sectional FIB-SEM images revealed the depths of the *t-m* transformed layer on mechanically pre-treated AlN and COJ surfaces to be approximately 3.68-4.00 µm and 4.71-5.88 µm, respectively (Fig 4).

DISCUSSION

The results of this study showed that there was no statistically significant difference in the bond strength between AlN and COJ groups under any aging conditions. Thus, the first hypothesis was rejected. After thermocycling, the bond strength of the AlN and COJ groups had decreased statistically significantly. Therefore, the second hypothesis was accepted.

The use of tribochemical silica treatment followed by silane coupling agent and composite cement application has been widely accepted as one of the benchmark pre-treatment techniques for cementation of zirconia-based restorations.[4,33] Tribochemical silica treatment creates a rougher surface on zirconia, providing a larger surface area and greater micromechanical interlocking with the composite cement.[29] Furthermore, the silica on the zirconia surface chemically bonds to silane, creating crosslinks with methacrylate groups of composite cement, thus providing additional bond strength.[23,24,29]

The FTIR and EDS analyses in this study confirmed the formation of Si-O-Si and Si-O-Al on the primed COJ surface by the presence of downshifts of Si-O peaks with enlarged bands (when compared to primer) around 1080 cm^{-1}, as well as an increase of C, O, and Si on the primed COJ surface. However, siloxane bonds possess low hydrolytic stability, which reduced the bond strength following thermocycling. These results are consistent with previous studies.[3,12,27,36]

The comparison of spectra obtained by FTIR showed that the differences between the primer and the primed COJ surface in the number, type, and position of vibrational compo-

Table 3 Elemental composition (%) of as-sintered zirconia, tribochemically silica-treated zirconia, tribochemically silica-treated zirconia plus RelyX Ceramic Primer, and nano-structured alumina-coated zirconia

Element	As-sintered zirconia	Tribochemically silica-treated zirconia	Tribochemically silica-treated zirconia plus RelyX Ceramic Primer	Nano-structured alumina-coated zirconia
Zr	57.0 (0.1)	58.8 (0.2)	44.3 (0.1)	58.8 (0.1)
O	30.5 (0.1)	29.6 (0.1)	34.4 (0.1)	27.1 (0)
Y	2.5 (0.1)	2.4 (0.1)	–	–
Hf	0.7 (0)	1.5 (0.1)	0.6 (0.1)	1.6 (0)
C	9.3 (0.1)	5.6 (0.2)	17.8 (0.1)	10.7 (0.1)
Al	-	0.9 (0)	1.1 (0)	1.8 (0)
Si	-	1.3 (0)	1.8 (0)	–

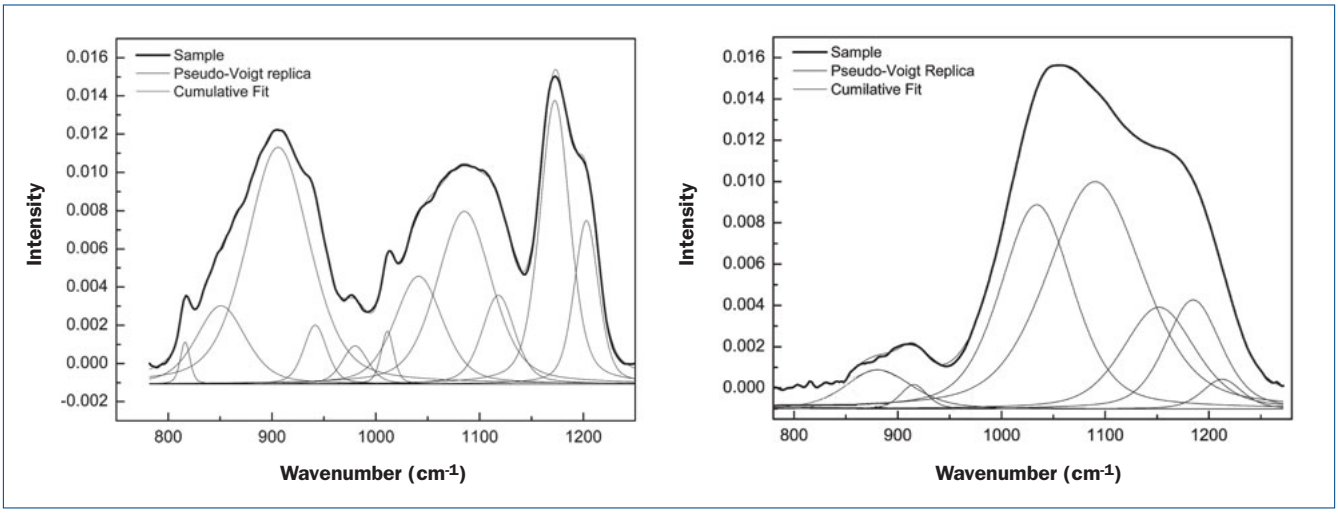

Fig 5 FTIR transmittance spectra of pre-treated zirconia surface and primer: a: RelyX Ceramic Primer; b: tribochemical silica treatment followed by RelyX Ceramic Primer.

nents are considerable. The spectrum of primer exhibited three strong bands in the region between 780 cm^{-1} and 1250 cm^{-1}, ie, area 1 between 800 cm^{-1} and 1000 cm^{-1}, area 2 between 1000 cm^{-1} and 1150 cm^{-1}, and area 3, a narrow band between 1150 cm^{-1} and 1250 cm^{-1} (Fig 5). Area 1 featured asymmetric Si-O-C stretching from $Si(OCH_3)n$ (n = 1, 2, 3)[12] and the contribution of Si-H stretching with much lower spectral intensity.[31] In area 2, vibrations from Si-O bonds were predominant, with the most intense component at ~1080 cm^{-1} arising from the Si-O-Si stretching. Two components in area 3, centered at ~1170 cm^{-1} and ~1200 cm^{-1}, can be assigned to C-O-C ester vibrations.[12] The primed sample, on the other hand, can be considered as comprising of one very weak band between 850 cm^{-1} and 950 cm^{-1} and a strong broad band between 950 cm^{-1} and 1250 cm^{-1}. The strong broad band can be considered as comprising primarily siloxane Si-O-Si stretching vibrations, with two pronounced components at ~1030 cm^{-1} and 1090 cm^{-1}.[11,31] The band strongly resembles silica-rich IR spectra documented in the literature.[37] However, the center of the whole broad band can be placed at ~1055 cm^{-1}, which is considerably lower than what would be expected if the vibrations arise from pure Si-O bonds. Lowering of the band center is indicative of the intermixing with the Al incorporation and the softening of vibrational frequencies due to the formation of Si-O-Al bonds.[37] The more Al is incorporated into the silica-rich layer, the more pronounced the decrease in overall band center is, due to an increase in the amount of mixed Si-O-Al bonding.

Jevnikar et al[17] have proposed the use of nano-structured alumina coating to increase surface area and wettability on zirconia surfaces as well as provide micromechanical interlocking with composite cement. A chemical interaction between the alumina coating and the zirconia surface is highly unlikely due to the inability of Al^{3+} to replace Zr^{4+} in

Table 4 Results of curve fitting

Parameters	Primer	Value	SE	Primed COJ	Value	SE
y_0	Peak1	-0.00107	0	Peak1	-0.00101	0
x_c	Peak1	816.40376	0.30563	Peak1	880.67061	0
A	Peak1	0.02759	0.00241	Peak1	0.18661	0.01817
w	Peak1	10.41147	0.87587	Peak1	77.79059	6.33954
mu	Peak1	0.5	0	Peak1	0.5	0
xc	Peak2	858.01637	3.54955	Peak2	915.47931	0.83532
A	Peak2	0.47345	0.08302	Peak2	0.04558	0.00506
w	Peak2	65.84905	3.08774	Peak2	30.47051	2.15702
xc	Peak3	906.18938	0.96133	Peak3	1033.97493	1.93608
A	Peak3	0.80516	0.15017	Peak3	1.03269	0.35138
w	Peak3	57.18443	6.28239	Peak3	82.33784	4.81525
xc	Peak4	940.98639	0.86621	Peak4	1090.27221	6.69635
A	Peak4	0.20911	0.06909	Peak4	1.52217	0.93624
w	Peak4	33.20226	4.28329	Peak4	109.00762	28.78334
xc	Peak5	980.25714	0.89113	Peak5	1151.8258	16.70235
A	Peak5	0.10189	0.01083	Peak5	0.5119	1.01631
w	Peak5	32.43738	3.44578	Peak5	81.90119	43.60575
xc	Peak6	1011.31833	0.41075	Peak6	1184.79783	7.75222
A	Peak6	0.06636	0.01096	Peak6	0.4245	0.61647
w	Peak6	16.21502	1.30073	Peak6	63.37112	23.72173
xc	Peak7	1038.77832	1.84234	Peak7	1212.79768	7.83052
A	Peak7	0.25812	0.13175	Peak7	0.08251	0.17396
w	Peak7	43.83635	7.25015	Peak7	45.1997	25.50262
xc	Peak8	1081.12176	2.42671			
A	Peak8	0.80475	0.27954			
w	Peak8	65.39794	14.90977			
xc	Peak9	1117.23339	1.33334			
A	Peak9	0.24318	0.13639			
w	Peak9	38.93912	6.79051			
xc	Peak10	1172.51609	0.24289			
A	Peak10	0.63997	0.01397			
w	Peak10	34.0313	0.48154			
xc	Peak11	1202.89221	0.33373			
A	Peak11	0.30326	0.0114			
w	Peak11	27.77709	0.79851			

y_0 = zero point (baseline); x_c = position (cm^{-1}); A = intensity; w = full width at half maximum; mu = pseudo-Voigt profile parameter; SE = standard error.

the crystal structure and the lack of sufficient appropriate interstitial spaces to accommodate Al^{3+} with its strong affinity towards tetrahedral coordination.[22,26,30]

SEM images of alumina coating showed a highly textured surface, which is favorable for micromechanical retention to composite cement (Fig 4). In addition, chemical bonding

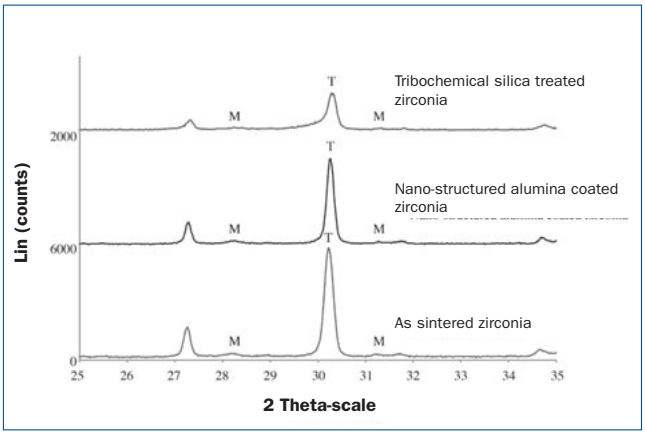

Fig 6 X-ray diffraction analyses of as-sintered, tribochemically silica-treated, and nano-structured alumina-coated zirconia. T indicates the tetragonal phase; M indicates the monoclinic phase.

between alumina and phosphate monomer in the composite cement is anticipated, although no primer was used (as proposed in the technique by Jevnikar et al[17]). However, given that the minimum thickness of the composite cement layer was 10 µm, no attempt was made to characterize the chemical bond, because the typical depth of infrared penetration in spectrometry cannot exceed 5 µm from the surface of the specimens, depending on wavenumber, incident angle, and refractive index of the ATR element.[18]

The failure modes of the AIN groups were predominantly adhesive or mixed. Since only resin matrices, not filler particles, were observed filling the intercrystal spaces of the alumina coating,[15] the fracture might possibly have occurred through this zone. The bond strength of AIN groups significantly decreased after thermocycling; however, the failure mode was not different compared to that reported for the short-term group.

Either mixed or cohesive failure in composite cement was observed in the COJ groups. A significant increase of adhesive and mixed failures was detected following thermocycling, suggesting that the siloxane bond was affected by the hydrolytic action of water and temperature variation.

When Weibull analysis is applied to bond strength studies, the greater the Weibull characteristic strength, the better the actual bonding effectiveness, and the greater the Weibull modulus, the less technique sensitive the bonding procedure is.[1] The Weibull characteristic strength and Weibull modulus values reported for the AIN and COJ groups were not statistically significantly different when compared together in each aging condition, indicating that the bonding efficacy and technique sensitivity of both groups were similar. However, the Weibull modulus and Weibull characteristic strengths of AIN groups decreased statistically significantly after thermocycling, while these values were not statistically significantly different in COJ groups (the 95% confidence interval of these groups overlapped when the statistical significance was calculated, as shown in Table 2), indicating that AIN specimens were more sensitive to thermocycling.

The preparation of the specimens involving air abrasion (COJ group) or soaking in aqueous solution at 70°C (AIN group) is responsible for *t-m* phase transformation of zirconia due to the energy of the impacting particles or low temperature degradation, respectively. Excessive *t-m* phase transformation would lead to the formation of a layer of compressive stresses on the zirconia surface, which would result in the formation of residual stresses within a few microns of depth from the interface and cause bond strength degradation.[28] Residual stresses may lead to strength degradation of zirconia and the bond; therefore, XRD and FIB-SEM were conducted to analyze the *t-m* phase transformation at the interface.

As mentioned above, soaking of AIN specimens in aqueous solution at 70°C is likely to cause *t-m* transformation as a result of low temperature degradation. On the other hand, following soaking, sintering of the nano-structured alumina coating layer is carried out at a temperature of approximately 900°C.[17] This temperature is sufficiently high to induce reversal of the phase transformation, and hence no *t-m* transformation should have been observed.[20] However, XRD analysis measured 3.33% monoclinic volume fraction for as-sintered zirconia, 4.2% in AIN specimens, and 6.16% in the COJ group (as expected due to air abrasion). It is noteworthy that the increase of monoclinic volume fraction is overall minimal. FIB-SEM was applied to measure the depth of the phase transformation (Fig 4). In FIB-SEM images, the transformed zone exhibited a smoother surface with twinning grain boundaries and the facetting of zirconia grains,[32] which allowed for direct measurement of the transformed layer.[2] In this study, the *t-m* transformed layer depth was measured within the range of 3.68 to 4.00 µm for AIN and 4.71–5.88 µm for COJ. The XRD and FIB-SEM confirmed that minimal *t-m* transformation occurred in all groups and that high temperature used for coating in AIN was unable to reverse the transformation, as also previously reported by Tholey et al.[32]

XRD analysis reported in Fig 6 shows an unidentified peak at approximately 2θ degree = 27°. Such a peak was consistently observed for all specimens. XRD mapping of the raw data of as-sintered zirconia specimens (group where the peak was more obvious) was conducted to identify the compound of the peak at 2θ degree = 27°. The possible compound should have related to the elements detected by EDS (Zr, Y, O, C, Hf) and/or to the composition of high translucent zirconia (HT zirconia) provided by GC (ZrO_2, Y_2O_3, HfO_2, Al_2O_3). However, none of the possible compounds which may have originated from these elements belongs to this peak. Additional analysis of XRD data of as-sintered specimens with a broader range approximately from 2θ degree = 25° to 80° (with a step size of 0.02 degrees and with a 1-s step interval) was conducted in order to identify another peak of the compound which may possibly match the peak at 27° did not provide any information. The presence of this peak was consistently found in all

tests we conducted with HT zirconia, suggesting that this peak is likely to be associated with the composition of this material and it is not a contaminant, nor is it associated with other materials which have been used for surface preparation. The presence of this peak was never recorded in our previous studies based on standard zirconia.[8,9] To our knowledge, the presence of this peak has also been reported only by Hallmann et al,[10] who examined the influence of blasting pressure and particle composition and size on the surface characterization of zirconia. The presence of this peak was not discussed by Hallmann et al,[10] and additional research is needed to understand the nature of this peak.

A study by Lee et al[21] reported that the shear bond strength between composite cement and alumina-coated zirconia was significantly higher than that of tribochemically silica-treated zirconia, when tested following water storage and thermocycling. These results contradict the results of the present study, where no statistically significant difference was observed between the two groups. In the study by Lee et al,[21] the characterization of the bond among the various groups was not investigated, making it difficult to interpret the differences between the two studies. However, the test methodology (shear bond strength test was used by Lee et al, whereas the microtensile bond strength test was employed in the present study) could partially explain the differences in the results.[21] This will be the subject of future studies.

In the present study, the influence of aging and hydrolysis was examined through thermocycling to a maximum of 10,000 cycles. The literature states that 10,000 cycles are comparable to 1 year of aging of an in-service restoration,[5] although the specimens are immersed in water for approximately 10 days. Temperature changes in the thermocycling process cause the materials to expand and contract cyclically; this process generates mechanical stresses at the bonded interface, resulting in bond strength degradation.[5] As a result of thermocycling, a significant decrease of the bond strength in both AIN and COJ groups was found. Other studies use different parameters, such as long water storage (from 6 months to 1 year). The outcomes following thermocycling or water storage may be different and caution should be exercised in comparing the results of different studies.

Alumina coating is commercially available in some countries. Following try-in of the restoration, the fitting surface can be effectively decontaminated with phosphoric acid without affecting the bond strength.[38] Other studies reported that the application of alumina coating showed significant higher bond strength and durability compared to air-abrasion techniques and potentially allows the use of zirconia in those clinical situations where bonding may be more challenging.[16,17,21] However, the present study did not confirm this. In addition, the application of alumina coating is currently time consuming when compared to more conventional techniques. The performance of alumina coating should be further investigated before recommending its clinical use.

CONCLUSIONS

The μTBS of AIN and COJ were not statistically significantly different. Thermocycling affected the bond strength of both groups. RelyX Ceramic Primer chemically reacted with tribochemically silica-treated zirconia. A tendency of failure mode to change from mainly cohesive to mainly mixed and adhesive was observed in the COJ groups following thermocycling, which might be indicative of a degradation of the siloxane bond. *T-m* phase transformation was found in both tested groups.

ACKNOWLEDGMENTS

This study was supported by the Australian Dental Research Foundation Inc., [grant no. RC/PC: E1405/RP549) and GC Corp. [grant no. RC E1512, Project no. D1387]. The authors are grateful to Mrs. Chanya Chuenarrom for her technical assistance in laboratory preparation. The authors acknowledge 3M Oral Care for supplying the materials used in this study. The authors also acknowledge Dr. Anna-Maria Erika Welsch for FTIR analysis as well as the facilities, scientific and technical assistance from the staff at the Sydney Analytical and Australian Microscopy and Microanalysis Research Facility (ammf.org.au), The University of Sydney. Dr. Putsadeeporn Thammajaruk gratefully acknowledges the Office of Higher Education Commission, Thailand, for the Strategic Scholarships Fellowships Frontier Research Network (specific for the southern region).

REFERENCES

1. Burrow MF, Thomas D, Swain MV, Tyas MJ. Analysis of tensile bond strengths using Weibull statistics. Biomaterials 2004;25:5031–5035.
2. Cattani-Lorente M, Scherrer S, Durual S, Sanon C, Douillard T, Gremillard L, Chevalier J, Wiskott A. Effect of different surface treatments on the hydrothermal degradation of a 3Y-TZP ceramic for dental implants. Dent Mater 2014;30:1136–1146.
3. Debnath S, Wunder SL, McCool JI, Baran GR. Silane treatment effects on glass/resin interfacial shear strengths. Dent Mater 2003;19:441–448.
4. Everson P, Addison O, Palin WM, Burke FJ. Improved bonding of zirconia substructures to resin using a "glaze–on" technique. J Dent 2012;40: 347–351.
5. Gale MS, Darvell BW. Thermal cycling procedures for laboratory testing of dental restorations. J Dent 1999;27:89–99.
6. Garvie RC, Nicholson PS. Phase analysis in zirconia systems. J Am Ceram Soc 1972;55:303–305.
7. Guazzato M, Albakry M, Ringer SP, Swain MV. Strength, fracture toughness and microstructure of a selection of all-ceramic materials. Part I. Pressable and alumina glass-infiltrated ceramics. Dent Mater 2004;20: 441–448.
8. Guazzato M, Albakry M, Ringer SP, Swain MV. Strength, fracture toughness and microstructure of a selection of all-ceramic materials. Part II. Zirconia-based dental ceramics. Dent Mater 2004;20:449–456.
9. Guazzato M, Quach L, Albakry M, Swain MV. Influence of surface and heat treatments on the flexural strength of Y-TZP dental ceramic. J Dent 2005;33:9–18.
10. Hallmann L, Ulmer P, Reusser E, Hämmerle CH. Effect of blasting pressure, abrasive particle size and grade on phase transformation and morphological change of dental zirconia surface. Surf Coat Technol 2012;206:4293–4302.
11. Hepburn C, Vale P, Brown A, Simms NJ, McAdam EJ. Development of online FTIR spectroscopy for siloxane detection in biogas to enhance carbon contactor management. Talanta 2015;141:128–136.
12. Hooshmand T, van Noort R, Keshvad A. Storage effect of a pre-activated silane on the resin to ceramic bond. Dent Mater 2004;20:635–642.
13. Inokoshi M, De Munck J, Minakuchi S, Van Meerbeek B. Meta-analysis of bonding effectiveness to zirconia ceramics. J Dent Res 2014;93:329–334.

14. ISO/TS:11405. Dentistry—Testing of adhesion to tooth structure. Geneva, Switzerland, 2015.
15. Jacobsen T, Söderholm K-J. Some effects of water on dentin bonding. Dent Mater 1995;11:132–136.
16. Jevnikar P, Golobič M, Kocjan A, Kosmač T. The effect of nano-structured alumina coating on the bond strength of resin-modified glass ionomer cements to zirconia ceramics. J Eur Ceram Soc 2012;32:2641–2645.
17. Jevnikar P, Krnel K, Kocjan A, Funduk N, Kosmac T. The effect of nano-structured alumina coating on resin-bond strength to zirconia ceramics. Dent Mater 2010;26:688–696.
18. Kazarian SG, Chan KA. ATR-FTIR spectroscopic imaging: recent advances and applications to biological systems. Analyst 2013;138:1940–1951.
19. Kern M. Bonding to oxide ceramics-laboratory testing versus clinical outcome. Dent Mater 2015;31:8–14.
20. Kosmac T, Oblak C, Jevnikar P, Funduk N, Marion L. The effect of surface grinding and sandblasting on flexural strength and reliability of Y-TZP zirconia ceramic. Dent Mater 1999;15:426–433.
21. Lee J-J, Choi J-Y, Seo J-M. Influence of nano-structured alumina coating on shear bond strength between Y-TZP ceramic and various dual-cured resin cements. J Adv Prosthodont 2017;9:130–137.
22. McCullough Jt, Trueblood K. The crystal structure of baddeleyite (monoclinic ZrO_2). Acta Crystallogr 1959;12:507–511.
23. Özcan M, Cura C, Valandro LF. Early bond strength of two resin cements to Y-TZP ceramic using MPS or MPS/4-META silanes. Odontology 2011;99:62–67.
24. Plueddemann EP. Adhesion through silane coupling agents. J Adhesion 1970;2:184–201.
25. Prasansuttiporn T, Thanatvarakorn O, Tagami J, Foxton RM, Nakajima M. Bonding durability of a self-etch adhesive to normal versus smear-layer deproteinized dentin: effect of a reducing agent and plant-extract antioxidant. J Adhes Dent 2017;19:253–258.
26. Putnis A. An introduction to mineral sciences. Cambridge: Cambridge University Press, 1992.
27. Queiroz JRC, Benetti P, Özcan M, de Oliveira LFC, Della Bona A, Takahashi FE, Bottino MA. Surface characterization of feldspathic ceramic using ATR FT-IR and ellipsometry after various silanization protocols. Dent Mater 2012;28:189–196.
28. Sato H, Yamada K, Pezzotti G, Nawa M, Ban S. Mechanical properties of dental zirconia ceramics changed with sandblasting and heat treatment. Dent Mater J 2008;27:408–414.
29. Senyilmaz DP, Palin WM, Shortall AC, Burke FJ. The effect of surface preparation and luting agent on bond strength to a zirconium-based ceramic. Oper Dent 2007;32:623–630.
30. Shannon RT, Prewitt CT. Effective ionic radii in oxides and fluorides. Acta Crystallogr B 1969;25:925–946.
31. Socrates G. Infrared and Raman characteristic group frequencies: tables and charts. Chichester: John Wiley & Sons, 2001.
32. Tholey MJ, Swain MV, Thiel N. SEM observations of porcelain Y-TZP interface. Dent Mater 2009;25:857–862.
33. Tzanakakis EG, Tzoutzas IG, Koidis PT. Is there a potential for durable adhesion to zirconia restorations? A systematic review. J Prosthet Dent 2016;115:9–19.
34. Vanderlei A, Bottino MA, Valandro LF. Evaluation of resin bond strength to yttria-stabilized tetragonal zirconia and framework marginal fit: comparison of different surface conditionings. Oper Dent 2014;39:50–63.
35. Wandscher VF, Fraga S, Pozzobon JL, Soares M, Zovico F, Foletto EL, May LG, Valandro LF. Tribochemical Glass Ceramic Coating as a New Approach for Resin Adhesion to Zirconia. J Adhes Dent 2016;18.
36. Wegner SM, Gerdes W, Kern M. Effect of different artificial aging conditions on ceramic-composite bond strength. Int J Prosthodont 2002;15:267–272.
37. Yu KMK, Thompsett D, Tsang SC. Ultra-thin porous silica coated silver–platinum alloy nano-particle as a new catalyst precursor. Chem Commun 2003:1522–1523.
38. Zhang S, Kocjan A, Lehmann F, Kosmac T, Kern M. Influence of contamination on resin bond strength to nano-structured alumina-coated zirconia ceramic. Eur J Oral Sci 2010;118:396–403.

Clinical relevance: Although the results of this study appear to indicate that nano-structured alumina coating has the potential to be an alternative method to tribochemical silica treatment, more studies are necessary to improve and optimize this technique prior to suggesting its clinical use.